IEEE Photonics Journal
An IEEE Photonics Society Publication

Haze and Polarization Scrambling of Nonlinearly Scattered Light From Antiglare Si Nanorod Surface

Volume 4, Number 1, February 2012

Gong-Ru Lin, Senior Member, IEEE
Yung-Hsiang Lin
Fan-Shuen Meng

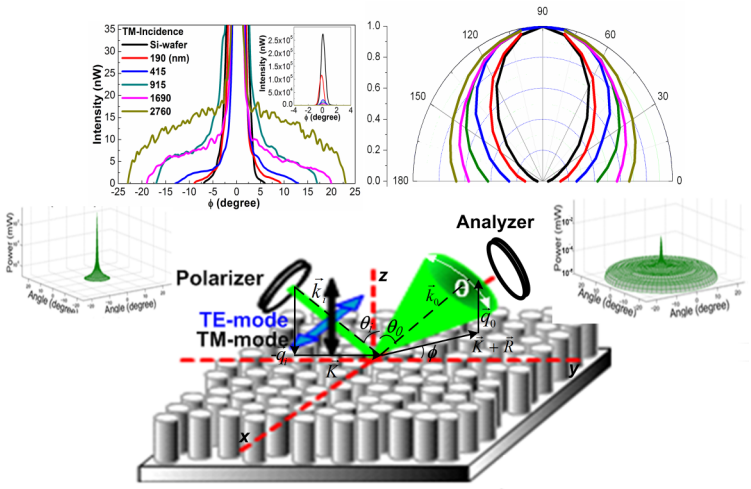

DOI: 10.1109/JPHOT.2012.2182762
1943-0655/$31.00 ©2012 IEEE

Haze and Polarization Scrambling of Nonlinearly Scattered Light From Antiglare Si Nanorod Surface

Gong-Ru Lin, *Senior Member, IEEE*, Yung-Hsiang Lin, and Fan-Shuen Meng

Graduate Institute of Photonics and Optoelectronics, Department of Electrical Engineering, National Taiwan University, Taipei 106, Taiwan

DOI: 10.1109/JPHOT.2012.2182762

Manuscript received November 24, 2011; revised December 30, 2011; accepted December 31, 2011. Date of publication January 4, 2012; date of current version January 24, 2012. This work was supported in part by the National Science Council, Taiwan, and the Excellent Research Projects of National Taiwan University, Taiwan, under Grant NSC98-2221-E-002-023-MY3, Grant NSC99-2622-E-002-024-CC2, and Grant NSC100-2623-E-002-002-ET. Corresponding author: G.-R. Lin (e-mail: grlin@ntu.edu.tw).

Abstract: The scattering angle, the Haze ratio, and the field polarization factor of the frequency-doubled Nd:YAG laser nonlinearly scattered from the semiconductor nanorod surface are investigated. Both the scattering angle and the reflected Haze ratio of the laser beam reflected from Si nanorod surface present a nonlinearly increasing trend with nanorod length. As the nanorod lengthens from 190 to 2760 nm, the scattering angle broadens from 2.5° to 25° and from 2.5° to 24°. Concurrently, the reflected Haze ratio increases from 5% to 22% and 3% to 21% under TE and TM-mode incidences, respectively. A significant polarization scrambling transfers the linearly polarization into an elliptical polarization, and the field polarization factor increases from 0.54 to 0.86 and from 0.42 to 0.84 under TE- and TM-mode incidences with an enlarging nanorod length from 190 to 2760 nm. The reflected Haze ratio is linearly proportional with the broadened scattering angle. However, the field polarization factor shows a gradually saturating effect at larger scattering angle. The theoretical calculation is used to quantitatively analyze the polarization scrambling effect, which demonstrates that the scattered wave nonlinearly depends on the surface corrugation and can be expressed by the second-order function of the surface corrugation strength. The strong correlations of the TE-mode scattering with the nanorod length and the TM-mode scattering with the laser incident angle are observed. The polarization of the reflected laser beam eventually transfers from a linear to an elliptical one with a nanorod length exceeding over 1 μm.

Index Terms: Scattering, nanostructures, optical and other properties.

1. Introduction

Nanoroughened structures have been considered to serve as an antireflective coating in the application of photovoltaic cells. Moreover, similar structures have also emerged to enhance the scattering and the Haze ratio on semiconductor surface to improve its photon absorption and optoelectronic conversion efficiency for energy transferring applications [1]–[5]. The low-dimensional nanorod surface with high aspect ratio and reduced refractive index is particularly interesting since it causes ultralow surface reflectance, unusual quantum confinement effect, optical emission extraction, and optical polarization, etc. [6], [7]. To approach the surface roughening, Morales and Lieber have employed the laser ablation-induced cluster formation and vapor–liquid–solid based chemical vapor deposition (VLS-CVD) technique to prepare uniformly distributed 30-μm-long single-crystal Si and Ge nanowires with diameters of 6–20 and 3–9 nm, respectively [8]. Yang *et al.*

demonstrated a directly colloid seeding VLS-CVD to grow vertically aligned single-crystalline Si nanowires with precisely controlled dimensions and spacing [9]. Peng *et al.* presented the aligned Si nanowire by etching the Si substrate with metal-particle mask [10], and several alternatives for Si nanorod formation were reported [11]–[13].

It was previously known that the polarized light could suffer from a multiple scattering in the inhomogeneous materials to cause polarization scrambling phenomenon which significantly impacts the spectroscopic and imaging performance [14], [15]. Mitzner has formulated the influence with simple surface scattering to explain the scattered light polarization scrambling from the roughened surface [16]. Renau *et al.* analyzed the correlation between surface backscattering and polarization scrambling [17], and some fundamentals have been realized via the modeling of the randomly scattered field with the variation of surface roughness [18], [19]. Other observations, such as the localized blur or obscured spot of visible light reflected from the nanoroughened surface obtained by using concentrated aqueous suspensions of the submicron polystyrene spheres, were also reported by Wolf and Maret [20]. The nanoroughened surface scattering-induced Haze and polarization scrambling enhancement play an important role in improving the photovoltaic cell efficiency. However, the corresponding theory or model has yet to be completely realized up to now.

In this paper, we investigate the scattering angle, the Haze ratio, and the field polarization factor of the frequency-doubled Nd:YAG laser nonlinearly scattered from the semiconductor nanorod surface, and a new small-perturbation field scattering model is established to quantitatively analyze the nanorod length dependency to the aforementioned phenomena. The enlarged Haze ratio and the field polarization factor of a linearly polarized laser nonlinearly scattered from the Si nanorod surface are characterized to realize the correlation between nanorod length and nonlinear field scattering. With small-signal perturbation, a modified field scattering model is established to simulate the nanorod length dependent laser beam blur, the maximum scattering angle, the Haze ratio, and the field polarization factor.

2. Experimental Setup

2.1. Preparation of Si Nanorods

In experiment, the large-area vertically aligned Si nanorods on (100)-oriented p-type Si wafer were obtained by wet-etching the Si wafer in aqueous $HF/AgNO_3$ solution with assistant nanoparticle metallic catalytic [10]. During the process, the Ag atoms were self-assembled into nanoparticles at the etching pores randomly allocated on the Si surface. Lengthening the etching time dissolves these pores deeply to form Si nanorods. Afterwards, the HNO_3 aqueous solution was employed to peel off the thick silver film wrapped around Si nanorods after the etching process. Fig. 1 illustrates the morphology of Si nanorod and plots its length and diameter as a function of etching time. Five samples were prepared by lengthening the etching duration in aqueous solution with the same concentration. The length of Si nanorods increases from 190 to 2760 nm with their diameters concurrently broadened from 42 to 51 nm as the etching time lengthens from 2 to 20 min.

2.2. Scattering Angle and Field Polarization Ratio Analyses

An incident light would suffer multiple scattering and spread the spot size from the Si nanorod roughened surface. In this case, the significant laser beam divergence occurs after it reflects from the Si nanorod roughened surface. Fig. 2(a) demonstrates the schematic diagram of reflected beam divergence. To investigate the effect of Si nanorod length on the surface nonlinear scattering, the divergent angle of the frequency-doubled Nd:YAG laser beam reflected from the Si nanorod samples, and the flat Si wafer under TE and TM-mode incidences were determined by using an experimental setup shown in Fig. 2(b). A continuous-wave laser with an optical power of 10 mW and passing through a linear polarizer is utilized to form the TE- and TM-mode incidences. The incident angle is 20°, and the distance between sample and power meter is 7 cm. An iris with a constant diameter of 250 μm was set in front of the power meter to spatially resolve the scattered beam power distribution. The nonlinearly scattered laser power as a function of the rotating angle is

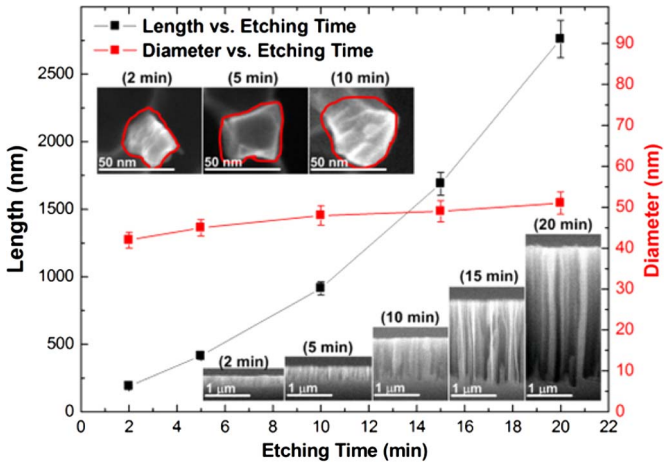

Fig. 1. Nanorod length and rod diameter versus etching time with the top-view and cross-sectional view of SEM images.

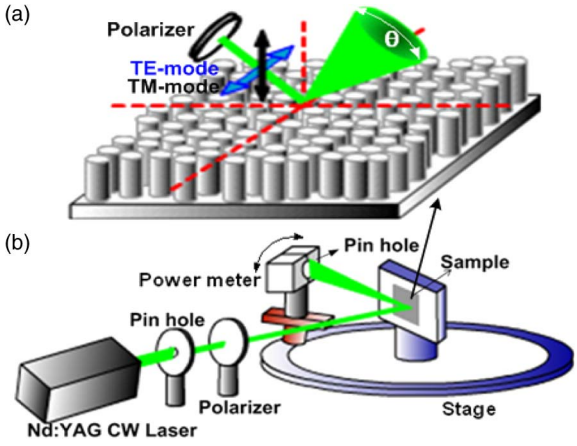

Fig. 2. (a) Schematic diagram of reflected beam divergence and (b) the experimental setup for scattering angle analysis.

plotted by consecutively scanning the power meter related to the reflected beam axis. After determining the degree of multiple scattering induced by the roughened surface, Fig. 3 demonstrates the field polarization factor measurement for the nonlinearly scattered laser reflected from the Si nanorod samples and the Si wafer with the same laser source under TE and TM-mode incidences at incident angle of 20°. An analyzer was inserted in front of the power meter to measure the polarization degree of the scattered laser beam. The field polarization factor of the nonlinearly scattered beam from the sample was detected by detuning the axis deviation between the polarizer and the analyzer from parallel to orthogonal.

3. Modeling the Field Polarization Factor of Nonlinear Scattered Laser Beam

To investigate the laser beam polarization scrambling induced by nonlinear scattering from the nanoroughened surface, we assume that a linearly polarized field with its wave vector $\vec{k}_i = (K_x, K_y, -q_{iz})$ and $\vec{K} = (K_x, K_y, 0)$ is incident on the sample surface (see Fig. 2), as expressed by $\vec{E}i(\vec{r}) = |Ei|\exp[i(K \cdot \mathrm{r} - q_i z)]$ with $\vec{E}i = (E_{ix}, E_{iy}, E_{iz})$ denoting a constant field vector and $\vec{r} = (r_x, r_y, z)$. The roughened Si nanorod surface is described by a surface corrugation function of $z = \alpha D(\vec{r})$ (where α represents the strength of the corrugation, i.e., the maximum nanorod length). The field polarization factor of $P_{\mathrm{TM/TE,TE}}(\vec{r})$ under TE-mode incidence $(E_{iy} = E_{iz} = 0)$ is

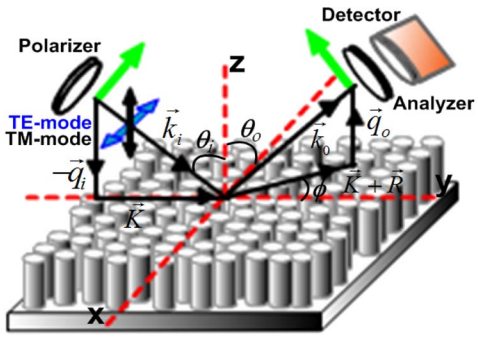

Fig. 3. Experimental setup for polarization scrambling analysis.

defined as the field ratio of the scattered TM to the TE component [18]. For a linearly polarized electromagnetic wave (considering TE-mode as an example), the field polarization factor approaches zero due to the condition of $E_{\mathrm{TM/TE}}(\vec{r}) \ll E_{\mathrm{TE/TE}}(\vec{r})$. The depolarization effect occurs after reflecting from the Si nanorod roughened surface and part of the field transfers to the TM-mode, which would lead to an increasing $E_{\mathrm{TM/TE}}$ component and a decreasing $E_{\mathrm{TE/TE}}$ component. In this case, the field polarization factor is degraded due to the depolarization effect.

Assume the scattered wave with wave vector $k_{\vec{R}} = (K_x + R_x, K_y + R_y, q_0)$ is collected at the plane of $\vec{K} + \vec{R}$, where $\vec{R} = (R_x, R_y, 0)$. With a small-perturbation, the field polarization factor in the incident plane with R_x approaching zero can be expressed as a function of Z_R, incidence angle, and azimuthal scattering angle [18]. By using the notations: $\sin\phi = R_x/[R_x^2 + (K + R_y)^2]^{1/2}$, $\cos\phi = (K + R_y)/[R_x^2 + (K + R_y)^2]^{1/2}$, $q_i = k_i\cos\theta_i$, $K = k_i\sin\theta_i$, and $q_o = k_o\cos\theta_o$, the field polarization factors under TE- and TM-mode incidences are expressed as

$$P_{\mathrm{TE}}(\vec{R}) = \left|\frac{E_{\mathrm{TM/TE}}(\vec{R})}{E_{\mathrm{TE/TE}}(\vec{R})}\right| = \left|\frac{\left[E_{ix}R_x^2 z_R\right]\frac{\sin\theta_i}{k_i^3} + R_x z_R(2\sin\theta_i)}{(k_i\cos\theta_i)z_R + i}\right| \tag{1}$$

$$P_{\mathrm{TM}}(\vec{R}) = \left|\frac{E_{\mathrm{TE/TM}}(\vec{R})}{E_{\mathrm{TM/TM}}(\vec{R})}\right| = \left|\frac{(i + k_o\cos\theta_o z_R)\sin\phi}{(i + k_i\cos\theta_i z_R)\cos\theta + 2R_y\sin\theta_i z_R}\right|. \tag{2}$$

From (1) and (2), it is expected that the field polarization factor will be gradually enlarged with increasing Z_R (Si nanorod length), and the field polarization factor is inversely proportional to the incident laser wavelength.

4. Results and Discussion

4.1. Nonlinear Scattering Angle of Laser Beam on Si Nanorod Surface

From our theoretical derivation, the linearly polarized laser beam could suffer a serious multiple scattering in the inhomogeneous material or on the nonuniform surface to cause a polarization randomization. In order to characterize the degree of surface roughness to the surface nonlinear scattering, the scattering angles of Si nanorod samples with different nanorod length are detected under TE and TM-mode incidences. Fig. 4 depicts the angular dependent power profiles of the laser scattered from the Si nanorod samples and from flat Si wafer. The 3-D schematic diagram is the scattered power distributions. The maximum power is located at the principle reflecting angle of the laser beam, which degrades rapidly with the angle increasing beyond 10°. The maximum scattering angle broadens from 2.5° to 25° and from 2.5° to 24° under TE and TM-mode incidences with increasing rod length from 190 to 2760 nm.

Previous works have clearly elucidated that the surface with longer Si nanorod greatly change its reflectance from constant to a depth dependent one which can be simulated with a multilayer structure [21]–[23]. Moreover, the severer light scattering process with larger laser beam

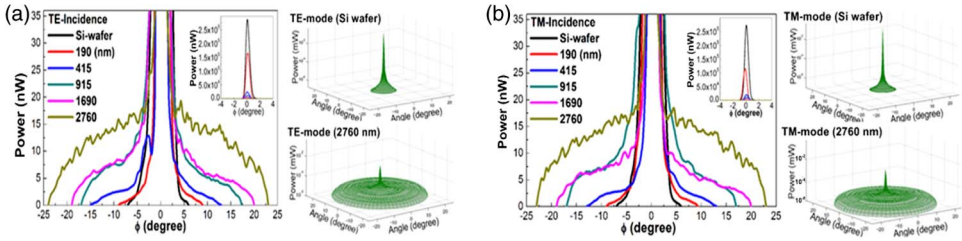

Fig. 4. Angular dependent nonlinearly scattered laser intensity measurement and the 3-D schematic diagram of the scattered power distribution under (a) TE and (b) TM-mode incidences with different nanorod length.

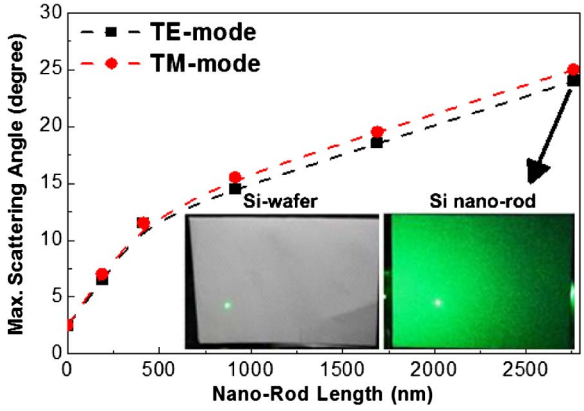

Fig. 5. Max. scattering angle versus nanorod length. Inset: the nonlinearly scattered laser spot patterns from Si wafer and 2.76 μm-long Si nanorod under TM-mode incidence.

divergence is also observed at longer nanorod sample. The optical wave of laser would penetrate deeper and suffer heavier multiscattering process, such that the beam divergent angle is greatly broadened (see Fig. 4). Such an effect is nearly polarization independent at very first characterization, providing the similar dependency of the scattering angle for TE- and TM-mode incidences with the nanorod length shown in Fig. 5. At the same detecting angle, the scattered laser intensity almost enlarges linearly with nanorod length but revealing a gradually saturation phenomenon as the nanorod lengthening to micrometer scale. Two inset pictures in Fig. 5 demonstrate the divergence of laser beam with greatly broadening scattering angle, in which the central part of the nonlinearly scattered laser beam pattern remains a Gaussian profile with a slightly broadened beam spot size. The polarization independences on the scattered beam spot size and maximum scattering angle are concluded.

4.2. Reflected Haze Ratio of Laser Beam Nonlinearly Scattered From Nanorod Surface

For practical applications in antireflective and antiglance photonic devices, the Haze ratio (light diffusivity/total transmittance) is utilized to define the degree of laser beam scattering from the roughened surface [3]. In the reflection case, the reflected Haze ratio (R_{Haze}) is defined as light diffusivity/total reflectance. To quantitatively characterize the degree of Haze ratio from the Si nanorod surface, the angular dependent scattering power is normalized to calculate the reflected Haze ratio as follows:

$$R_{\text{Haze}} = (P_{\text{rod}} - P_{\text{Si-wafer}})/P_{\text{rod}} = \int_0^{\pi}\int_{-\theta}^{\theta} \left\{ \left[\frac{P_{\text{rod}}(\theta)}{P_{\text{rod}}(0)} - \frac{P_{\text{Si-wafer}}(\theta)}{P_{\text{Si-wafer}}(0)}\right] \Big/ \left[\frac{P_{\text{rod}}(\theta)}{P_{\text{rod}}(0)}\right] \right\} d\theta\, d\phi \qquad (3)$$

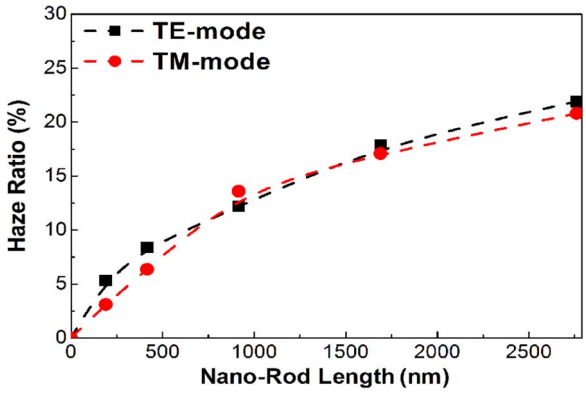

Fig. 6. Reflected Haze ratio of laser beam nonlinearly scattered from Si nanorod samples and Si wafer under TE and TM-mode incidences.

where P_{rod} and $P_{Si\text{-}wafer}$ denote the normalized reflecting laser power integrated over the whole scattering angle.

The light diffusivity from a flat Si wafer is less as compared with that from a Si nanorod roughened surface, therefore, the difference of light power detected from the Si nanorod surface, and the Si wafer represents the light diffusivity. The subtraction of P_{rod} by $P_{Si\text{-}wafer}$ with remaining scattering distribution accurately characterize the effect of surface multiple scattering on the reflected Haze ratio. According to the definition of (3), high Haze ratio indicates the increasing light diffusivity or the decreasing reflectance. With the enhanced nonlinear scattering by surface nanorods, a larger Haze ratio with its value gradually saturating at micrometer-long nanorod scale is obtained. Fig. 6 reveals that the reflected Haze ratio increases from 5% to 22% and from 3% to 21% with nanorod lengthening from 190 to 2760 nm under TE- and TM-mode incidences, respectively. The similar trend between scattering angle and reflected Haze ratio of laser beam nonlinearly scattered by lengthened Si nanorod is confirmed, which essentially provides a designer's rule to optimize the nanorod length property for compensating aforementioned effects with the degraded transparency simultaneously.

4.3. Field Polarization Factor of Laser Beam Nonlinearly Scattered From Nanorod Surface

On the other hand, the significant multiple scattering occurred at Si nanorod surface also induces a polarization scrambling effect on the reflected beam of a frequency-doubled Nd:YAG laser. The polarization scrambling by Si nanorod with different nanorod lengths is huge, compared with that by the flat Si substrate shown as a function of the rotating angle of analyzer in the polar-coordinate plots of Fig. 7(a) and (b), and the field polarization factor of the samples with different nanorod lengths under TE- and TM-mode incidences are demonstrated in Fig. 7(c). In comparison, the TE-mode incidence suffers a more serious polarization scrambling from the spatially confined nanorod top surface, whereas the TM-mode incident laser beam falls within the vertically aligned Si nanorod to slightly release the mixed substrate effect. In principle, either the multiple scattering or the multiple reflections from an inhomogeneous dielectric material can have a significant impact on the polarization scrambling effect [24]. This phenomenon can be analyzed by comparing the field polarization factor of the reflected laser beam, as defined by the ratio of the transferred polarized field to the original polarized field. By lengthening the nanorod length from 190 to 2760 nm, the field polarization factor gradually increases from 0.54 to 0.86 for the TE-mode incident laser beam and from 0.42 to 0.84 for the TM-mode incident laser beam.

Both the TE- and TM-mode laser incidences partially transfer into their orthogonally polarized components when suffering from the nonlinear scattering among Si nanorods, which detune a linearly polarized laser beam to an elliptically polarized one. The experimental observations indicate

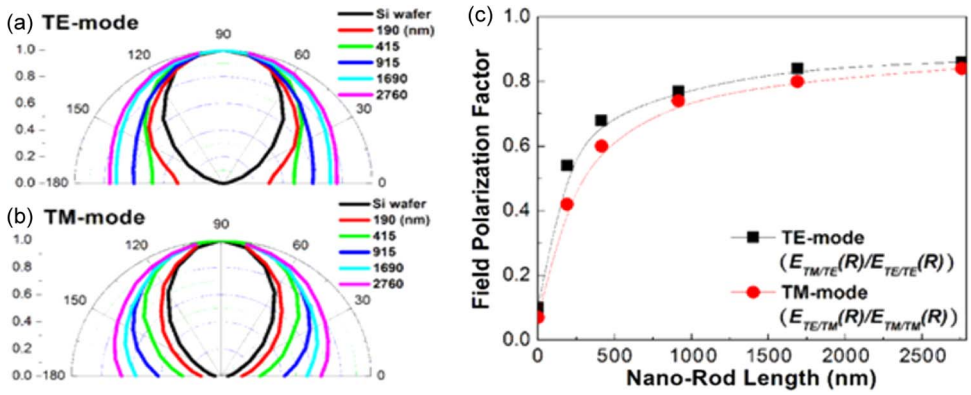

Fig. 7. Depolarized reflection in polar coordinate under (a) TE and (b) TM-mode incidences. (c) Complex filed polarization factor versus nanorod length in TE and TM-mode incidences.

that the field polarization factor of the TE-mode laser incidence increases seriously than TM-mode laser incidence, which results from the direction of the electric field of TE-mode is perpendicular to the nanorod structure, hence experiencing a more roughened structure than TM-mode [22]. From the analytical results given by (1) and (2), it is evident that the surface nanorod corrugation induces an additional scattering term on the induced TM-mode reflection transfer from the original TE-mode with a proportionality to the second-order corrugation amplitude or the sequence of the maximum nanorod length. In comparison, the laser ellipsometry can also be used to analyze the ratio of reflection coefficient (r_{TM}/r_{TE}) and the phase variation for those surface nanoroughened samples by using the following equation:

$$\frac{r_{TM}}{r_{TE}} = \frac{E_{TM,r}}{E_{TM,in}} \times \frac{E_{TE,in}}{E_{TE,r}} = \tan\varphi \exp(i\Delta) \tag{4}$$

where E_r and E_{in} represent the electric field of the reflected wave and the incident wave. The φ and Δ are measured to determine the ratio of reflection coefficient and the phase difference. For our sample with nanorod length of 190 nm, the φ and Δ are determined as 55.63° and 173.55°, respectively. The phase difference can confirm that the reflected light is elliptically polarized [24]. To correlate with our experimental data, the field polarization factors under TE- and TM-mode incidences are taken into calculation. For TE-mode incidence, $E_{TM,r}/E_{TE,r} = 0.54$ and $E_{TE,in}/E_{TM,in} = 2.02$, φ'_{TE} is 47.46°. For TM-mode incidence, $E_{TE,r}/E_{TM,r} = 0.42$ and $E_{TM,in}/E_{TE,in} = 2.04$, φ'_{TM} is 49.23°. The deviation of the ϕ value results from the different polarizer used in the ellipsometry and our experimental setup, which changes the value of $E_{TE,in}/E_{TM,in}$. That is, the variation on the amplitude ratio of the orthogonally polarized components $(E_{TM,r}/E_{TE,r})$ under different polarized incident wave can also be investigated from our analysis with changing polarization of incidence.

4.4. Comparison on Simulated and Experimental Field Polarization Factor

The roughened surface formed by Si nanorods would induce the perturbation on the electric field of the scattered laser beam. The depolarized reflection from such a roughened surface can be well described by extinction theory, providing the complex field polarization factor as a nonlinear function of surface corrugation in the relationship with the second-order expansion of the scattered field [18]. According to the theoretical model derived in the former section, the field polarization factor is verified to exhibit a saturation trend with nanorod lengthening up to 500 nm or longer. Fig. 8(a) and (b) are the comparisons between the simulation and the experimental field polarization factors under TE and TM-mode laser incidences, respectively. The simulation results correlate well with the experimental results, except that the deviation occurred at shorter nanorod length region.

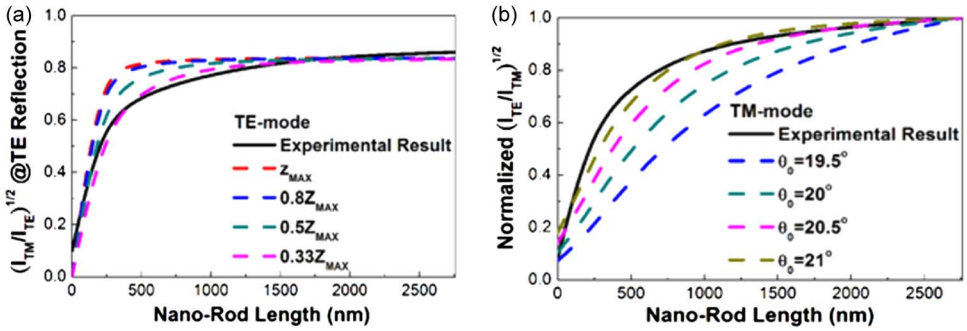

Fig. 8. (a) Simulation curves with different z_R (accompanying with the reduction of surface corrugation factor from z_{MAX} to 0.33 z_{MAX}). (b) Simulation curves with changing incident angles.

During the simulation of TE-mode laser incidence, the surface corrugation Z_R is assumed to be the maximum nanorod length. However, the randomly distributed size of the self-aggregated Ag nanocatalyst [25] and the different dissolving rate of each etching pore have led to the nonuniform length and size distribution of Si nanorod, such that Z_R should be modified by a factor which represents an average nanorod length taken into consideration of the real case. In addition, the Si nanorods is affected not only by the length but also by the area density of the Si nanorods under TE-mode illumination. The area density of the Si nanorods (number of nanorods per unit area) is decreased with increasing etching time in these samples. Since the self-aggregated Ag particles (the etching pore) at deeper region become larger to collapse the longer Si nanorods, which inevitably produce numerous vacancies among the Si nanorod array formed by lengthening the etching time. In experiment, the increase of the randomly collapsed regions result in a reduced area density of the Si nanorods when lengthening the etching time, which leads to a deviation between the experimental and simulating results. As shown in Fig. 8(a), the experimental curve of the field polarization factor versus nanorod length gradually deviates from the simulation curve using the maximum surface corrugation Z_R. The effective Z_R for optimizing the TE-mode simulation is observed to decrease from 0.8 to 0.33 with concurrently increasing Si nanorod length and reducing area density. For example, four simulation curves are employed to show their coincidence with the experimental curve at different nanorod lengths. After modification, our simulations show good agreement with the experiments for samples with long Si nanorods by decreasing the surface corrugation. For the simulation under TM-mode laser incidence, the field polarization factor is strictly dependent on the incident angle of the laser beam. The polarization of TM-mode is located in the incidence plane in parallel with the orientation of the Si nanorods vertically aligned on the substrate surface. The simulation reveals that even a tiny incident angle variation of TM-mode incidence would greatly influence the interaction area of laser electric field and the Si nanorod surface. Fig. 1(b) elucidates that the experimental curve of the normalized field polarization factor can only be perfectly matched by our simulation with a slightly modification on the incidence angle from 19.5° to 21°.

To further investigate the correlation of evolution of Haze ratio and polarization scrambling with the roughened surface induced multiple scattering, two diagrams shown in Fig. 9 have depicted the reflected Haze ratio and the field polarization factor as a function of the scattering angle. In Fig. 9(a), it is straightforward that the reflected Haze ratio is linearly proportional with the broadened scattering angle. However, the field polarization factor of the reflected laser beam from the nanorod corrugated surface shows a gradually saturating effect at larger scattering angle. Therefore, both the Haze ratio and the polarization scrambling degree for the reflected laser beam from the Si nanorod surface show a good correlation with the surface nonlinear scattering effect. The quantitative analyses demonstrate that the Si nanorod surface would induce abundant multiple scattering and reflection, but a saturated polarization scrambling effect occurs after scattering from the longer Si nanorods. Both the simulation and the experimental data approach a maximum field polarization factor (i.e., the maximum polarization scrambling) under TE and TM-mode incidences,

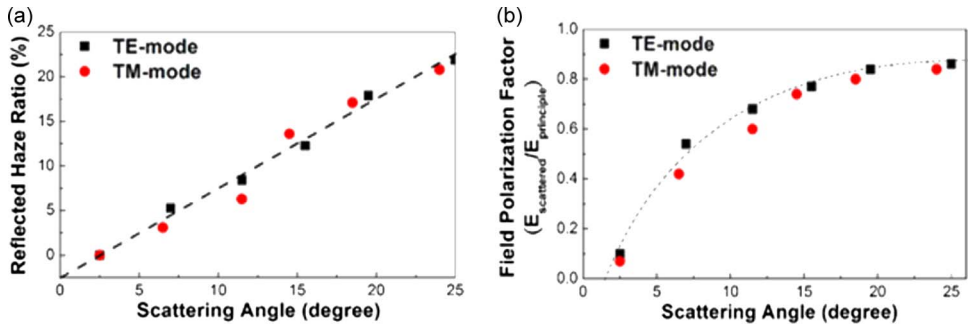

Fig. 9. (a) Diagram of the reflected Haze ratio versus scattering angle and (b) the diagram of field polarization factor versus scattering angle.

the existence of the asymptote can be determined by approaching the limit of (1) and (2), as follows:

$$\lim_{z_R\to\infty} P_{\mathrm{TE}}(\vec{R}) = \left|\frac{\left[(E_{ix}R_x)\frac{1}{k_i^2} + 2k_i\right]R_x\tan\theta}{k_i^2}\right| \tag{5}$$

$$\lim_{z_R\to\infty} P_{\mathrm{TM}}(\vec{R}) = \left|\frac{q_o\sin\phi}{k_i\cos^2\theta + 2R_y\sin\theta}\right|. \tag{6}$$

According to the theoretical model, the linearly polarized laser incidence is perturbed by the roughened surface, the scattering field thus becomes the elliptically polarized one after interaction with the severely roughened surface. The maximum polarization scrambling occurs when the field polarization factor approaches 1, such that the reflected laser beam transfers the elliptical polarization to nearly circular polarization. By enlarging the value of Z_R to infinity, the Z_R term in (1) and (2) can be eliminated, which interprets that the field polarization factors under TE- and TM-mode laser incidences are independent with the surface nanorod corrugation when the nanorod exceeds over a critical length. This observation suggests an optimized length of more than 1 μm for optimizing the surface nonlinear scattering induced Haze and polarization scrambling, since a longer nanorod will inevitably degrade the transmittance to compromise the antiglare and transparency of the nanorod corrugated surface [26]. In contrast, the field polarization factor linearly increases with enhanced surface corrugation sensitively when the nanorod is much shorter than a critical length of 500 nm. As a result, the scattering field of the reflected laser beam is presented in the second order of the strength of the surface corrugation, which simultaneously induces the beam broadening and the polarization scrambling effects to enhance the Haze ratio and the polarization scrambling on the incident laser beam with a saturating trend to the scattering angle.

5. Conclusion

In conclusion, we investigate the scattering angle, the Haze ratio, and the field polarization factor of the frequency-doubled Nd:YAG laser nonlinearly scattered by the semiconductor nanorod surface. Due to the surface corrugation-dependent nonlinear multiple scattering, both the scattering angle and the reflected Haze ratio of the laser beam reflected from the Si nanorod surface present a nonlinearly increasing trend with nanorod length. With the nanorod lengthening from 190 to 2760 nm, the maximum scattering angles broaden from 2.5° to 25°, and from 2.5° to 24°, the reflected Haze ratios increase from 5% to 22% and 3% to 21% under TE and TM-mode laser incidences, respectively. The reflected Haze ratio reveals a saturating trend with lengthening nanorod and exhibits a linear proportionality with the scattering angle. The theoretical calculation based on the Ewald-Oseen theory is used to quantitatively analyze the polarization scrambling effect of the

reflected laser beam nonlinearly scattered by the Si nanorod surface. A significant polarization scrambling transfers the linearly polarized laser incidence into an elliptical polarization, and the corresponding field polarization factor nonlinearly increasing by lengthening nanorod is observed. By lengthening the nanorod from 190 to 2760 nm, the field polarization factor of a linearly polarized laser beam nonlinearly scattered from the Si nanorod surface increase from 0.54 to 0.86 and from 0.42 to 0.84 under TE and TM-mode laser incidences. The polarization of the reflected laser beam eventually transfers from linear to elliptical one after scattering by extremely long nanorod. The polarization scrambling effect of the scattered wave nonlinearly depends on the surface corrugation and can be expressed by the second-order function of the corrugation strength. The strong correlations of the TE-mode scattering with the nanorod length and the TM-mode scattering with the laser incident angle are observed. With a nanorod length exceeding over 1 μm, both the theoretical simulation and experimental observation confirm that the polarization scrambling effect saturates as the reflected laser beam has became elliptically polarized with its field polarization factor approaching maximum. The optimized nanorod length is therefore confined within 0.5–1 μm to compromise the scattering induced Haze ratio and the degraded transparency of the reflected laser beam.

References

[1] I. Gonzalez-Valls and M. Lira-Cantu, "Vertically aligned nanostructures of ZnO for excitonic solar cells: A review," *Energy Environ. Sci.*, vol. 2, pp. 19–34, 2009.

[2] C. Lin and M. L. Povinelli, "Optical absorption enhancement in silicon nanowire arrays with a large lattice constant for photovoltaic applications," *Opt. Exp.*, vol. 17, no. 22, pp. 19 371–19 381, Oct. 2009.

[3] S. S. Lo, D. Haung, and D. J. Jan, "Haze ratio enhancement using a closely packed ZnO monolayer structure," *Opt. Exp.*, vol. 18, no. 2, pp. 662–669, Jan. 2010.

[4] Y. C. Chao, C. Y. Chen, C. A. Lin, and J. H. He, "Light scattering by nanostructured anti-reflection coatings," *Energy Environ. Sci.*, vol. 4, no. 9, pp. 3436–3441, 2011.

[5] Q. Gan, H. Hu, H. Xu, K. Liu, S. Jiang, and A. N. Cartwright, "Wavelength-independent optical polarizer based on metallic nanowire arrays," *IEEE Photon. J.*, vol. 3, no. 6, pp. 1083–1092, Dec. 2011.

[6] M. L. Kuo, Y. J. Lee, T. C. Shen, and S. Y. Lin, "Large enhancement of light-extraction efficiency from optically pumped nanorod light-emitting diodes," *Opt. Lett.*, vol. 34, no. 13, pp. 2078–2080, Jul. 2009.

[7] M. Kobayashia and T. Hiramoto, "Experimental study on quantum confinement effects in silicon nanowire metal–oxide–semiconductor field-effect transistors and single-electron transistors," *J. Appl. Phys.*, vol. 103, no. 5, p. 053709, Mar. 2008.

[8] A. M. Morales and C. M. Lieber, "A laser ablation method for the synthesis of crystalline semiconductor nanowires," *Science*, vol. 279, no. 5348, pp. 208–211, Jan. 1998.

[9] A. I. Hochbaum, R. Fan, R. R. He, and P. D. Yang, "Controlled growth of Si nanowire arrays for device integration," *Nano Lett.*, vol. 5, no. 3, pp. 457–460, Mar. 2005.

[10] K. Peng, H. Fang, J. Hu, Y. Wu, J. Zhu, Y. Yan, and S. T. Lee, "Metal-particle-induced, highly localized site-specific etching of Si and formation of single-crystalline Si nanowires in aqueous fluoride solution," *Chem. Eur. J.*, vol. 12, no. 30, pp. 7942–7947, Oct. 2006.

[11] G. B. Jung, Y. J. Cho, Y. Myung, H. S. Kim, Y. S. Seo, J. Park, and C. Kang, "Geometry-dependent terahertz emission of silicon nanowires," *Opt. Exp.*, vol. 18, no. 16, pp. 16 353–16 359, Aug. 2010.

[12] X. Liu and D. Wang, "Kinetically-induced hexagonality in chemically grown silicon nanowires," *Nano Res.*, vol. 2, no. 7, pp. 575–582, 2009.

[13] Y. H. Pai, Y. C. Lin, J. L. Tsai, and G.-R. Lin, "Nonlinear dependence between the surface reflectance and the duty-cycle of semiconductor nanorod array," *Opt. Exp.*, vol. 19, no. 3, pp. 1680–1690, Jan. 2011.

[14] D. J. Pine, D. A. Weitz, P. M. Chaikin, and E. Herbolzheimer, "Diffusing wave spectroscopy," *Phys. Rev. Lett.*, vol. 60, no. 12, pp. 1134–1137, Mar. 1988.

[15] G. Maret and P. E. Z. Wolf, "Multiple light scattering from disordered media. The effect of Brownian motion of scatterers," *Z. Phys. B, Condens. Matter*, vol. 65, pp. 409–413, 1987.

[16] K. M. Mitzner, "Change in polarization on reflection from a tilted plane," *Radio Sci.*, vol. 1, pp. 27–29, 1966.

[17] J. Renau, P. K. Cheo, and H. G. Cooper, "Depolarization of linearly polarized EM waves backscattered from rough metals and inhomogeneous dielectrics," *J. Opt. Soc. Amer.*, vol. 57, no. 4, pp. 459–461, Apr. 1967.

[18] M. N. Vesperinas, "Depolarization of electromagnetic waves scattered from slightly rough random surfaces: A study by means of the extinction theorem," *J. Opt. Soc. Amer.*, vol. 72, no. 5, pp. 539–547, May 1982.

[19] J. J. Sein, "A note on the Ewald-Oseen extinction theorem," *Opt. Commun.*, vol. 2, no. 4, pp. 170–172, Sep. 1970.

[20] P. E. Wolf and G. Maret, "Weak localization and coherent backscattering of photons in disordered media," *Phys. Rev. Lett.*, vol. 55, no. 24, pp. 2696–2699, Dec. 1985.

[21] Y.-F. Huang, S. Chattopadhyay, Y.-J. Jen, C.-Y. Peng, T.-A. Liu, Y.-K. Hsu, C.-L. Pan, H.-C. Lo, C.-H. Hsu, Y.-H. Chang, C.-S. Lee, K.-H. Chen, and L.-C. Chen, "Improved broadband and quasi-omnidirectional anti-reflection properties with biomimetic silicon nanostructures," *Nat. Nanotechnol.*, vol. 2, no. 12, pp. 770–774, Dec. 2007.

[22] G.-R. Lin, F. S. Meng, Y. H. Pai, Y. C. Chang, and S. H. Hsu, "Manipulative depolarization and reflectance spectra of morphologically controlled nano-pillars and nano-rods," *Opt. Exp.*, vol. 17, no. 23, pp. 20 824–20 832, Nov. 2009.

[23] O. L. Muskens, J. G. Rivas, R. E. Algra, E. P. A. M. Bakkers, and A. Lagendijk, "Design of light scattering in nanowire materials for photovoltaic applications," *Nano Lett.*, vol. 8, no. 9, pp. 2638–2642, Sep. 2008.
[24] E. Hecht, *Optics*. San Francisco, CA: Addison-Wesley, 2002.
[25] G.-R. Lin, C. J. Lin, H. C. Kuo, H. S. Lin, and C. C. Kao, "Anomalous microphotoluminescence of high-aspect-ratio Si nanopillars formatted by dry-etching Si substrate with self-aggregated Ni nanodot mask," *Appl. Phys. Lett.*, vol. 90, p. 143102, Apr. 2007.
[26] G.-R. Lin, Y. H. Pai, and C. T. Lin, "Microwatt MOSLED using SiOx with buried Si nanocrystals on Si nano pillar array," *J. Lightwave Technol.*, vol. 26, no. 11, pp. 1486–1491, Jun. 2008.